Preferred citation: G. Bellani, R. Bach, F. Lundell and L.D. Söderberg. Experimental study of filtration of fiber suspensions: Part II: combined PIV and pressure drop measurements. In **Advances in Pulp and Paper Research, Oxford 2017**, *Trans. of the XVIth Fund. Res. Symp. Oxford, 2017*, (W. Batchelor and D. Söderberg, eds), pp 281–298, FRC, Manchester, 2018. DOI: 10.15376/frc.2017.1.281.

EXPERIMENTAL STUDY OF FILTRATION OF FIBER SUSPENSIONS

PART II: COMBINED PIV AND PRESSURE DROP MEASUREMENTS

Gabriele Bellani[1], Roland Bach[1], Fredrik Lundell[1] and L. Daniel Söderberg[1,2]

[1] Linné Flow Centre, KTH Mechanics, SE-100 44 Stockholm, Sweden
[2] Innventia AB, SE-114 86 Stockholm, Sweden

ABSTRACT

The filtration of a fiber suspension has been studied experimentally. Typical applications where pressure filtration occurs are: papermaking, air cleaners, production of composite materials, etc. In particular, in papermaking, the quality of the final product depends on the fiber orientation and mass distribution in the filtered material. Micro-variations of these properties can strongly affect the quality of the final product and they can occur during filtration, thus it is important to predict how this can happen. However, this is not an easy task, first because the filtered cake is a non-homogeneous compressible porous media, second because the filtration flow is non-stationary, since the cake is continuously evolving in time. Therefore in this work we focus on the filtration flow through formed steady fiber networks. For each grammage (*i.e.* mass of fibers per unit area), we simultaneously measure the pressure drop across the network and velocity field on top and below the fiber network using Particle Image Velocimetry (PIV). Compression of the fiber network can also be extracted from the (PIV images. Normalized filtration resistance was found to be decreasing with increasing network thickness, as well as network compressibility. From the PIV data the influence of the formed fiber network on the flow field was analyzed and characteristic scales of the flow structures are quantified.

1 INTRODUCTION

Pressure filtration is the process by which a suspension of particles is forced to flow through a filter medium, so that particles larger than the characteristic size of the filter are separated from the fluid. This is of interest for a wide range of applications such as car filters, production of composite materials [14, 4], gas cleaners [5], papermaking [6], etc. During filtration, particles will clog the filter medium, often forming a cake of filtered material on top of it, thus altering the filtration efficiency. In many applications it is important to accurately predict the evolution of the pressure drop and of the retention capabilities during the filter clogging. Depending on the operating pumps, filtration can occur at fixed rate/variable pressure or at constant pressure/variable rate. Filtration processes are one part of the very general field of separation of solids from a liquid. Its fundamentals can be found in the flow through a porous medium, which can be quantified with Darcys Law. Further processes are sedimentation and thickening, centrifugation and consolidation [3]. The theory of filtration is connected to the development and the applications of thickening. The origin of modern sedimentation and thickening is based on a theory by [8], and extended to pressure filtration by [2]. Their assumption is that the relative local velocity between solids and the liquid is only a function of the solids volumetric concentration ϕ. These models describe the evolution of the cake build up process and the filter-cake resistance as a function of time. However the models are based on average equations for the solid concentration, which do not take into account inhomogeneities in the filter cake. Instead, in applications like papermaking it is of great interest to be able to describe in detail the development of the filtered cake, since in this case, the cake itself is the final product [11]. Even though sometimes retention properties and microstructure of the network can strongly be affected by chemistry and additives [9], several experimental investigation showed that the micro structure of the fiber network (distribution of mass and fiber orientation) can be modified by the filtration flow, see [13, 10] for details. However, the mechanism by which these phenomena can occur has never been investigated systematically. It is well known that regions of high strain and vorticity can modify the orientation of a fiber [7], and it has been shown that these regions can appear on top of the filter cake during filtration [1] by the inhomogeneous distribution of gaps in the fiber network. This can induce and change velocity gradients in the flow, which in turn can modify the distribution of the next layer of fibers.

1.1 Aim of this work

The presented work is part of an experimental program that deals with filtration of fiber suspensions. It can be seen as a continuation of the experimental study of

the formation of a fiber network from [1], but it is performed with a different experimental method. In the previous study the flow structures in a continuous filtration process were analyzed. Velocity measurements have been performed in the close proximity of the forming fiber network, thus providing insights in the small scales of the flow. Since the continuous filtration of a fiber suspension is highly non-stationary, the flow analysis is very complicated due to the complex interactions between the forming network and the filtration flow. The challenge is to perform filtration experiments in an appropriate way, so that we can get new insights in the flow characteristics that describe the unsteady filtration and network forming process. The fact that the flow field changes very quickly in the continuous filtration of a fiber suspension led to the idea to change the experimental method in a way to overcome the involved measurement issues. In the previous work measurements have been done while the fiber network was forming whereas in this thesis we want to study the flow structures over steady fiber networks to decouple the complex interactions which arise in the filtration process. That means that, after we have formed a fiber network of a defined grammage, we study the flow where the carrier fluid flows through the steady fiber network. Given that we will analyze the network forming process and the characteristic flow structures at different (steady) formation stages, we can easily acquire long time-series of data to ensure good statistics. The study of the hydrodynamic effects of steady fiber networks on the filtration flow allows us to investigate the governing characteristics in an easier way. We perform PIV measurements with a high spatial resolution in order to detect the relevant small scales in the filtration process. Compared to the previous work the studied flow region is enlarged to the width of the filtration apparatus, so that also the large scales can be properly measured. Further, we combined the PIV

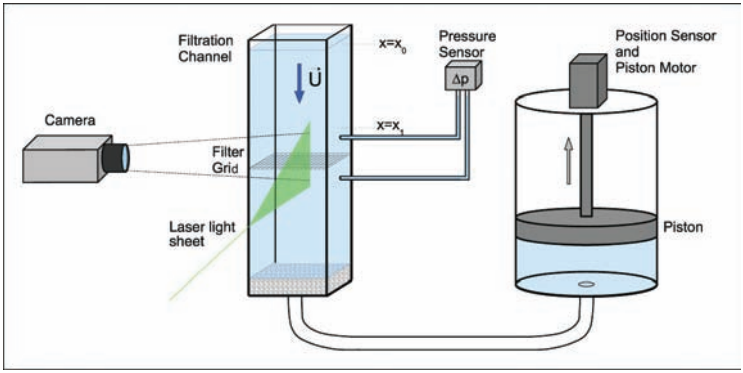

Figure 1. Sketch of the experimental setup and the measurement devices.

technique with pressure measurements, to quantify the pressure drop over the steady fiber networks. A scaling of the filtration resistance that is independent of network thickness will also be proposed here.

2 EXPERIMENTAL METHOD

2.1 Setup

The filtration of a fiber suspension and the forming process of a fiber network is studied in a vertical channel. The channel is built in acrylic for optical access to the flow to allow the PIV measurements. The channel has a cross-sectional area $S = 80 \times 80$ mm^2 and a length of 700 mm. A grid is installed at the half of the channel length and acts as filter in the experiment. The grid has a wire diameter of $d_m = 1$ mm and a spacing of $s_G = 2$ mm. Figure 1 shows a sketch of the filtration apparatus and the measurement devices for pressure and PIV measurements. The channel is opened on top, to be able to add the fibers to the fluid and to move them out of the channel after they have been filtered on the grid. The flow is generated by a motor-driven piston, which moves in an external fluid reservoir. Depending on its moving direction, the fluid is pushed into the vertical channel (filling phase) or sucked out of it (filtration phase). The actual position of the free surface of the fluid inside of the channel is coupled to the piston and is monitored by a position sensor. The filtration velocity only depends on the supply voltage of the piston motor. A calibration has been done and allows to set the motor voltage to achieve the desired flow velocity. The highest flow velocity in this configuration is approximately 85 mm/s. The reference coordinate system inside of the channel has its origin on the filtration grid. The *x*-axis is in the filtration direction and the *y*-and *z*-axis define the plane in which the filtration grid is positioned. The

Table 1. Parameters for the channel and the fiber suspension

Fibers:	density	$\rho_F = 1.8$ g/cm^3
	length	$l_f = 9.4$ mm
	diameter	$d_f = 0.26$ mm
Fluid:	density	$\rho_0 = 1.17$ g/cm^3
	viscosity	$\mu_0 = 1.52 \cdot 10^{-3}$ Pa · s
Channel:	cross-section	$S = 80 \times 80$
	length	$L = 700$ mm
Filtration grid:	wire diameter	$d_M = 1$ mm
	grid spacing	$S_G = 2$ mm

Table 2. Non-dimensional parameters for the experiments and the papermaking process

	Experiments	*Papermaking*
Re_{dM}	0.8–5	4–15
Re_{df}	0.2–1.3	0.8–3

coordinate system is shown in Figure 2. Table 3.1 gives an overview of the parameters from the channel and the fiber suspension in the experimental setup.

2.2 Fiber suspension

The fibers are made of Fluorocarbon, a synthetic flexible material of density $\rho_f = 1.8$ g/cm^3. The length of the fibers used in these experiments is $l_f = 9.4$ mm and the diameter is $d_f = 0.26$ mm. Thus the fiber aspect ratio is $r_f = l_f/d_f \approx 36$.

The suspending fluid is a solution of 65% glycerine and 35% water, with a resulting density $\rho_0 = 1.17$ g/cm^3 and a viscosity of $\mu_0 = 1.52 \cdot 10^{-3}$ Pa·s. A summary of the characteristics scales and physical properties of fluid, fibers and experimental setup are summarized in Table 1. Based on the scales we just described, we can define three non-dimensional parameters: the already mentioned fiber aspect ratio r_f, the Reynolds number based on the wire diameter $\mathrm{Re}_{d_M} = \dfrac{\rho_o U_\infty d_M}{\mu_0}$, and the Reynolds number based on the fiber diameter $\mathrm{Re}_{d_f} = \dfrac{\rho_o U_\infty d_f}{\mu_0}$. The combination of physical scales and fluid viscosity chosen for the experiments allow us to be in a range of Reynolds numbers that are reasonably close to that of papermaking applications, as reported in Table 2.

2.3 Measurement techniques

The pressure drop across the fiber network was estimated with a differential pressure sensor with a sensitivity of 60 Pa/Volt. The sensor specifications are summarized in Table 3.

Velocity measurements were performed using 2-dimensional PIV. The system was made of a high-speed camera with a CCD-sensor of 1024 × 1024 pixels resolution, a bit depth of 12 bits and a maximum frame rate of 4000 fps at full resolution. The measurement area, of size 80 × 80 mm^2 located at the center of the channel (as shown in Figure 2) was illuminated by a continuous wave green laser (532 nm, from LASER 2000). Due to the limited speed of the flow, the exposure time could be controlled by the camera shutter, thus no additional shutter

Table 3. Specifications of the pressure sensor

Pressure Range	0–250 Pa
Supply Voltage	5 V
Full Scale Span	4V at 250 Pa
Max. Total Error	±3% of full span

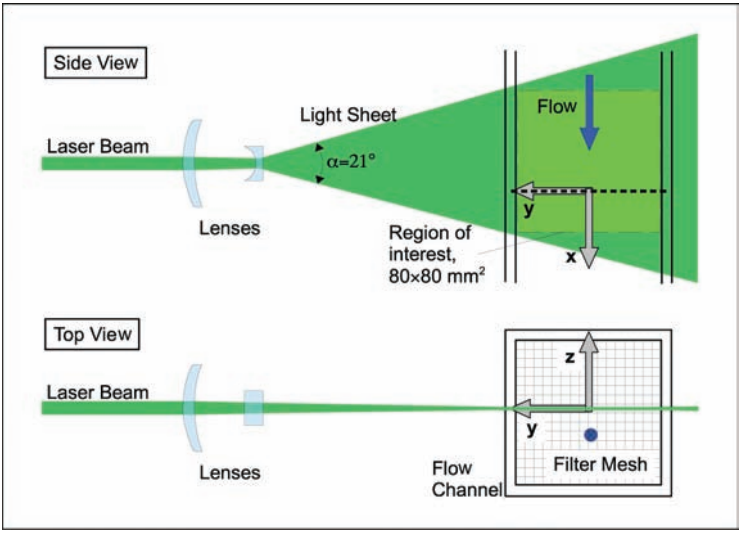

Figure 2. Measurement area and coordinate system.

on the laser was needed. The software *DaVis 7.2* from *LaVision GmbH* was used for image acquisition and processing. The algorithm used was a continuous window deformation and reduction, which allowed us to compute velocity fields of 341 × 341 vectors with a spatial resolution of about 0.225 × 0.225 mm^2.

The raw image acquired by the high-speed camera could also be used to track the network height during filtration.

2.4 Experimental procedure

At first a fiber network with a defined fiber grammage on top of the grid in the channel has to be created. Therefore the channel if filled with the glycerine-water solution until the free surface of the liquid has reached the start position $x = x_0$ (I).

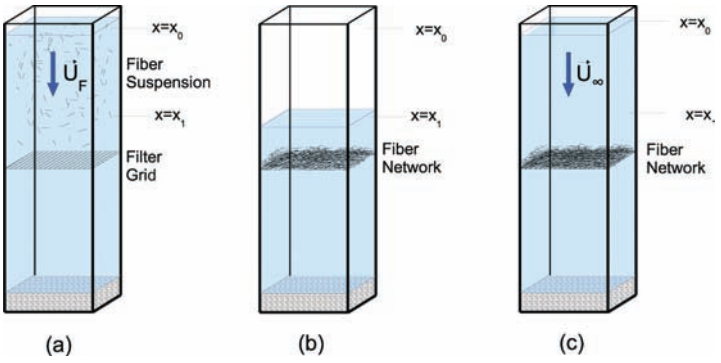

Figure 3. Forming and filtration of a steady fiber network. Network forming with U_F, start at $x = x_0$ (a), stop the formation at $x = x_1$ and refill the channel slowly (b), start the filtration over the steady fiber network with U_∞ (c).

Then a weighted amount of fibers is added to the fluid (II) and mixing is started immediately after that (III). A long stick is used to mix the solution to generate a fiber suspension with a homogeneous fiber distribution. The stirring is done manually and great care is taken not to create large coherent structures during the mixing process. The mixing is done for about 10s and the filtration starts immediately after that, so that no sedimentation can occur in between. The suspension is filtered with velocity U_F until the free surface of the liquid has reached the end position $x = x_1$ (IV). Once this is done, the channel is refilled again up to the start position $x = x_0$ (V). The refilling is performed at a very low flow rate, to keep the previously formed fiber network in its actual state. The network is now prepared and the actual measurements can start. From this point, the filtration of the liquid through the fiber network can be performed at a filtration velocity $U\infty$. Simultaneously, the pressure sensor acquires the pressure drop over the fiber network and the camera acquires particle images from the filtration flow (VI). This experimental procedure can be summarized by the following steps (and illustrated in Figure 3):

I. Fill the channel until the fluid has reached the start position x_0.
II. Add fiber mass according to the fiber grammage to test (fiber grammage is defined as mass of fibers per unit area).
III. Stir the suspension until a homogeneous fiber distribution is reached.
IV. Form a fiber network with forming velocity U_F, stop at end position x_1.
V. Refill the channel slowly to the start position x_0
VI. Run the filtration experiment over the steady fiber network with filtration velocity U_∞ and acquire flow data, stop at end position x_1.

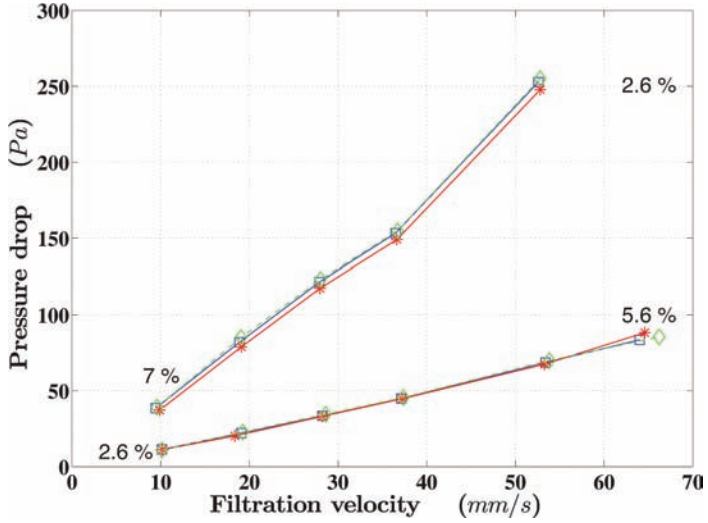

Figure 4. Pressure drop over the fiber network depending on the filtration velocity. The deviations from the repetition tests are given in percent for the grammages of 156g/m^2 (*below*) and 1875g/m^2 (*above*).

Step V and VI can be repeated in order to obtain statistics. The fibers are then removed out from the channel. Then the procedure I–VI is repeated either with a different fiber grammage or a different forming velocity on the same fiber grammage. In order to check the repeatability of the process we just described, experiments with two grammages and six different filtration velocities were performed. Each case was repeated three times, creating a new fiber network each time. Pressure drop was measured for each case and the results are shown in Figure 4. The three realizations agree with each other very well for all cases, with a maximum variability of the order of 5%.

3 RESULTS

3.1 Pressure drop

Data on the pressure drop for each filtration velocity and fiber grammage are acquired during step (VI) as described above. The sampling frequency of the time-resolved pressure signal was adjusted so that the free surface in the channel moved approximately 1 mm in the vertical direction in between two samples.

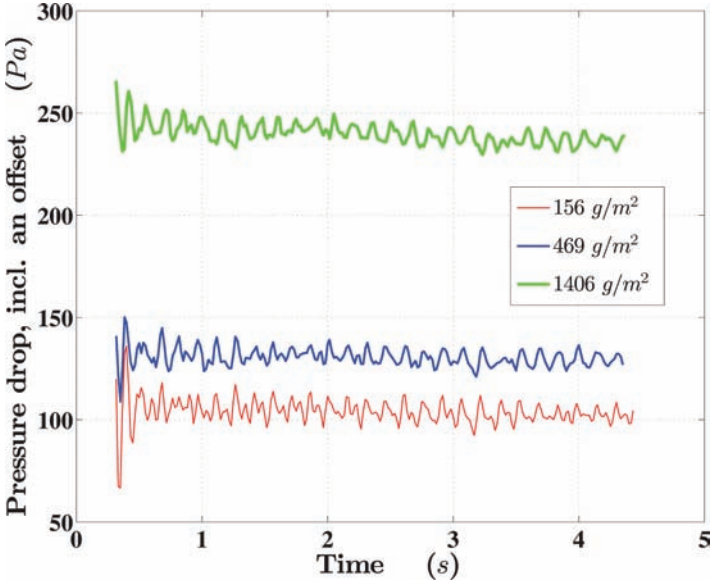

Figure 5. Acquired raw data of the pressure sensor at filtration velocity U_∞ = 52.9 mm/s for three fiber grammages: 156 g/m^2 (red), 409 g/m^2 (blue) and 1406 g/m^2 (green).

Typical time series acquired during three realizations are shown in Figure 5. The startup of the piston leads to some pressure oscillations, thus this part is not used for the statistics. An important observation is that the pressure signal is basically constant (except from small pressure oscillation due to noise and/or vibrations), so in our experiments both pressure and filtration rate can be considered to be constant.

Average pressure drop for 36 experimental cases, corresponding to 6 filtration velocities and 6 fiber grammages are shown in Figure 6(a). The error bars represent the standard deviation of the mean over three realizations and are shown for clarity only for the lowest and the highest fiber grammage. The first impression is that the pressure drop increases linearly with the grammage, at least within the accuracy of our measurements. It is interesting to observe that the linearity can be extended down to 0 grammage, i.e., we did not observe a steep increase in pressure drop from the empty grid to the case where the first layer of fibers are deposited as reported by other researches. The solid symbols represent the case where the network has been formed with a different formation velocity (U_F, see step IV). No significant effect of U_F on the pressure drop has been found.

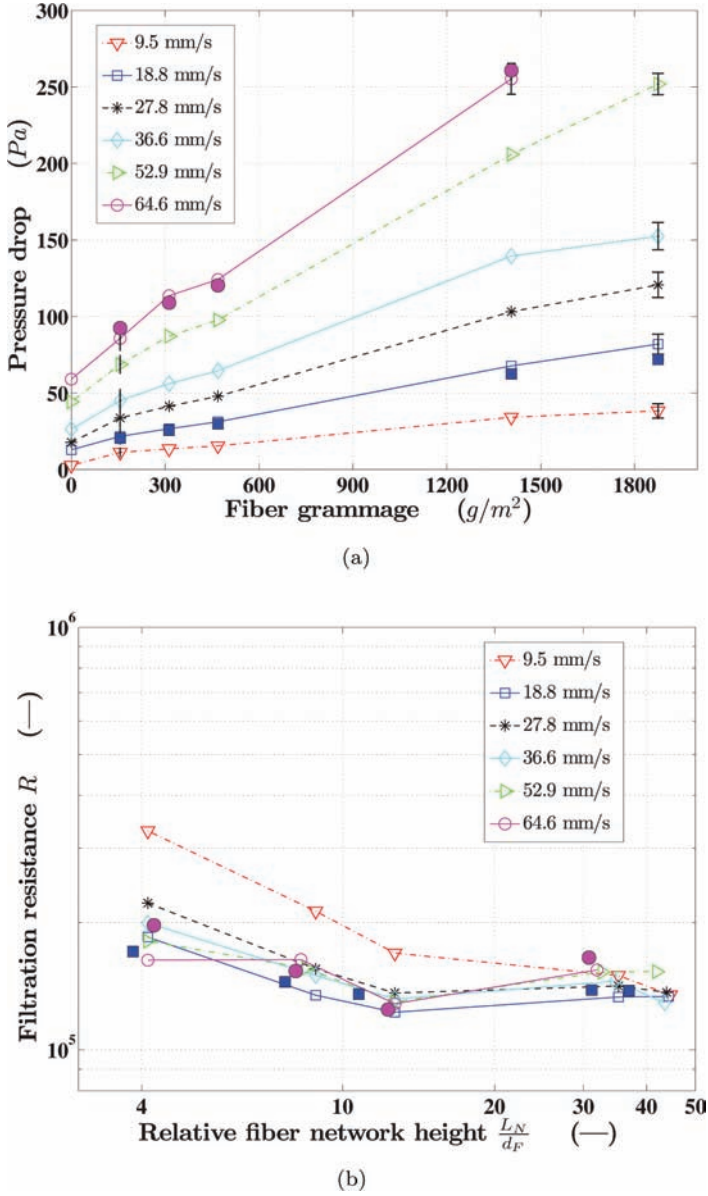

Figure 6. Dimensional (a) and non-dimensional (b) filtration resistance R over a steady fiber network for different filtration velocities.

To compare all different measurements, the data is presented in a scaled form in Figure 6(b). Here a non-dimensional filtration resistance R is shown as a function of the relative network height for different filtration velocities. The filtration process in our setup can be considered as an one-dimensional flow and Darcys Law becomes:

$$U \approx K \frac{\Delta p}{\mu L} \Rightarrow \frac{1}{K} = \frac{\Delta p}{\mu_0 U_\infty L_N} \left[\frac{1}{\mathrm{m}^2} \right] \tag{1}$$

The height of the studied porous media is given by L_N and denotes the averaged height of the fiber network. L_N is coupled to the fiber grammage w and the occurring network compression during filtration, respectively. The measured pressure drop over the fiber network is Δp and μ indicates the fluid viscosity. The filtration velocity in our experiment is given by U_∞. Based on the one-dimensional form of Darcys Law in equation (1) we can multiply the term $1/K$ (with the permeability coefficient K, given in m^2) with the cross-sectional area S of our filtration channel, to get a non-dimensional form of the pressure drop. The filtration resistance R is then defined by:

$$R \sim \frac{1}{K'} \quad R = \frac{\Delta p S}{\mu_0 U_\infty L_N} \tag{2}$$

The filtration resistance R in a study from the flow through a pulp pad was estimated to be in the order of $R \approx 10^7 - 10^8$, with a measured pressure drop of about 20 kPa [12]. The evaluation of L_N, which includes the effect of network compression, is explained in subsection 5.3. On the x-axis in Figure (3), we replace the fiber grammage w with the non-dimensional parameter L_N/d_F (where d_F is the fiber diameter). The curves for the different filtration velocities are very close to each other due to the scaling and it shows the similarity.

3.2 Flow field

In this paragraph we present results from the PIV measurements of the filtration flow. PIV measurements were performed for two filtration velocities (18.8 and 64.6 mm/s) and 6 fiber grammages. For each case we acquired about 900 image pairs from which instantaneous snapshots of the flow field could be computed. However, since the flow is stationary, we can average the instantaneous flow fields and get a more accurate description of the flow structures generated at the different stages (i.e, at different grammages) of the filtration process.

To distinguish between the different test cases we use the following nomenclature: $\bar{U}_{i,j}$, where $i \in [l, h]$ indicates one of the two forming velocities (l: low, h:

high), and the index $j \in [0, 1, 2, 3, 4, 5]$ indicates the fiber grammages w (g/m^2). The corresponding values for the filtration velocities are given in Table 4.

Figure 7 shows the contours of the mean velocity fields. Velocities are normalized by the corresponding mean filtration velocity U_F. Figures 7(a) and 7(b) show the velocity fields over the empty grid for low and high velocity, respectively. As expected, a thicker boundary layer is present at the channel walls for the lower filtration velocity, however this will not effect further quantitive analysis, since only the central part of the channel will be considered. There are regions of high and low speed both above and below the grid. The resulting regions of high strain can in principle modify the orientation of the incoming flow and in both cases they extend approximately one d_M.

Figures 7(c)–(f), show the velocity fields above and below a fiber network of increasing grammage. The black area over the grid indicates to the fiber network. The average height is computed by thresholding the raw images. Note that compression effects are evident in that the network formed at higher velocity (left) is thinner than for the low velocity. Already at low grammage flow structures much larger than for the case of the empty grid are formed. These structures affect the flow both below and above the grid, however differences between the two filtration velocities are more apparent downstream the grid.

A way to quantitively compare the results and objectively define the region where the flow is affected by the network is to introduce the function:

$$\bar{U}_{rms,y}(x)\sqrt{\frac{1}{Ny}\sum_{i=1}^{N_y}(\bar{U}(y_i x)-\bar{U}_y(x))^2} \tag{3}$$

where N_y is the number of data points in the horizontal direction and $\bar{U}_y$ is the mean flow velocity at given vertical position x averaged in y. $\bar{U}_{rms,y}(x)$ is maximum close close to the network (where the velocity profiles are maximally distorted by the high and low speed regions) and decreases away from it to reach a minimum where the velocity profiles are flat. It is assumed that the flow field is

Table 4. Nomenclature for the test cases and underlying test parameters

i, j	$i \rightarrow U_F$ (mm/s)	k	k$\rightarrow w$ (g/m^2)
l (low)	18.8	0	0
h (high)	64.6	1	156
		2	312
		3	469
		4	1406
		5	1875

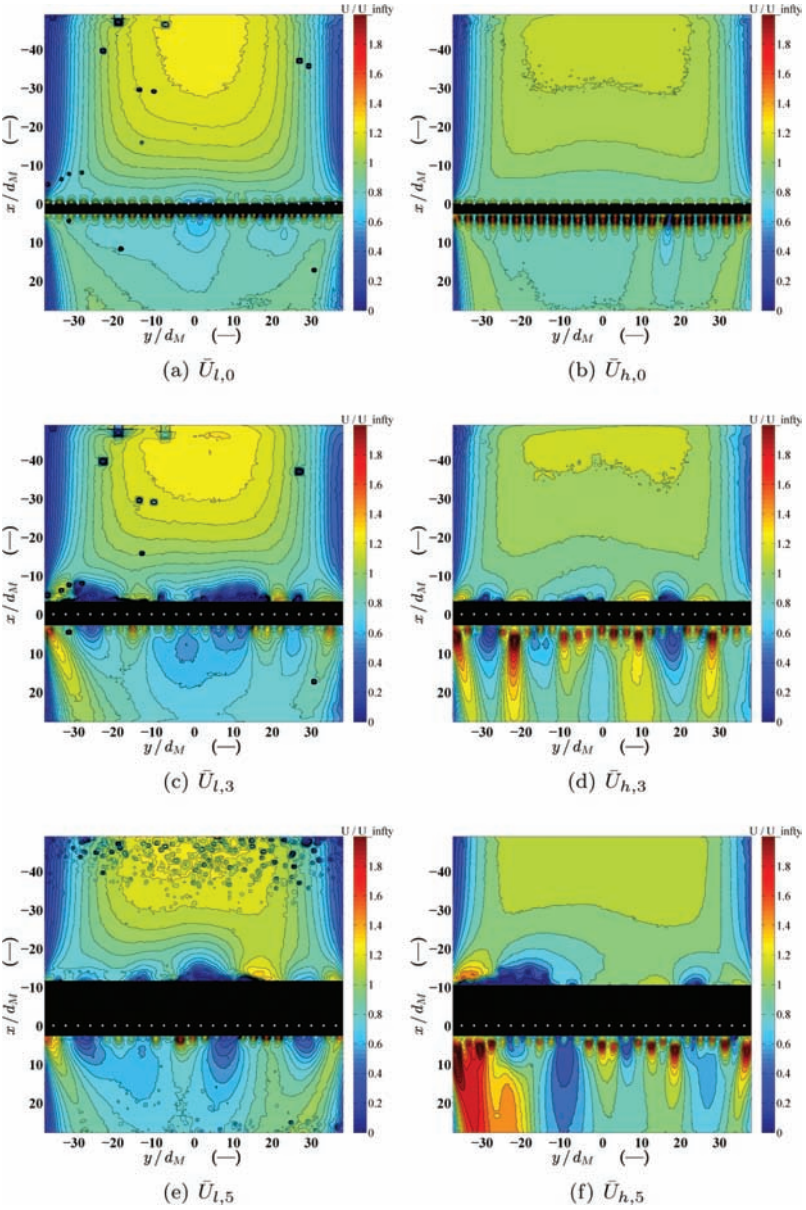

Figure 7. Normalized mean flow velocity $\bar{U}$ for U_∞ = 18.8 mm/s ((a), (c), (e)) and for U_∞ = 64.6 mm/s ((b), (d), (f)) for fiber networks of different grammages. The grid is shown by the white dots and the fiber network above is indicated by the black area.

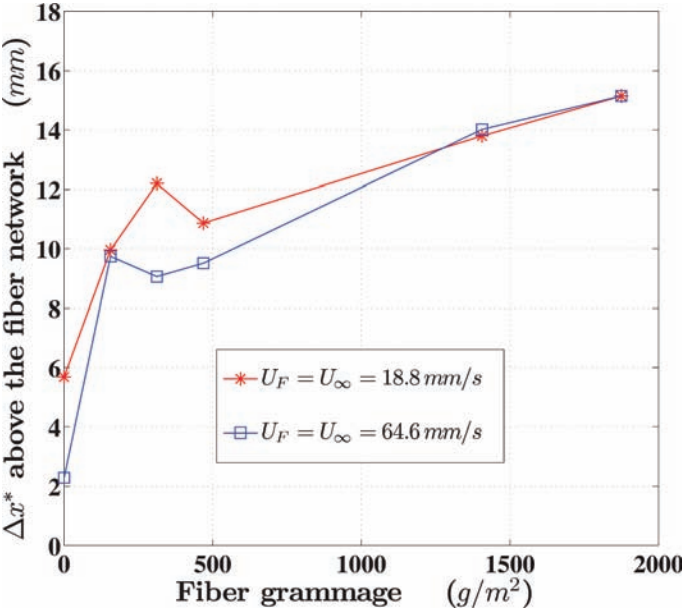

Figure 8. Extracted heights of the influenced region above the fiber network. The filtration velocities are U_∞ = 18.8 mm/s and 64.6 mm/s.

affected by the network until this minimum is reached. The distance between the top of the fiber network to the minimum of Eq. (3) is Δx^*. Figure 8 shows Δx^* for all the cases. The figure confirms that the influenced region increases rapidly when the first fiber layer is deposited on the grid, but then it grows slowly with a nearly linear slope. Interestingly, the effect of the filtration velocity seems to be negligible.

In Figure 9 we present the power spectra of the horizontal velocity profiles. They help us quantify the scales of the velocity variation in the horizontal direction, and hence the scales over which velocity gradients can act to rotate a fiber. The first thing we notice is a peak corresponding to $\lambda \approx 4$mm (i.e., the grid spacing) below the grid for both velocities. This means that no matter how thick the fiber network is, the signature of the mesh is always present (this is empirically confirmed by the so called wire mark on real paper). This peak is smoothed out above the network, where the scales are independent of the mesh size, and generally larger. Some peaks are shown for $3\text{mm} < \lambda < 8\text{mm}$, which is of the same order as the fiber length. However there are no significant differences for the different filtration rates and/or fiber grammages.

3.3 Network compression

The network height can be tracked in time from the PIV images. Figure 10(a) shows the time evolution of the network height for low and high filtration velocity at fiber grammge $w = 1875$ g/m^2. The network height is expressed as percentage of the initial height (defined as 100% at $t = 0$, just before the flow is started). It can be seen that as soon as the filtration starts the network is compressed. The network height remains constant during filtration. The total compression is 14% for the highest filtration velocity. Interestingly, considerable compression (12%) occurs also for the lowest velocity. After the filtration ends, the network tends to recover

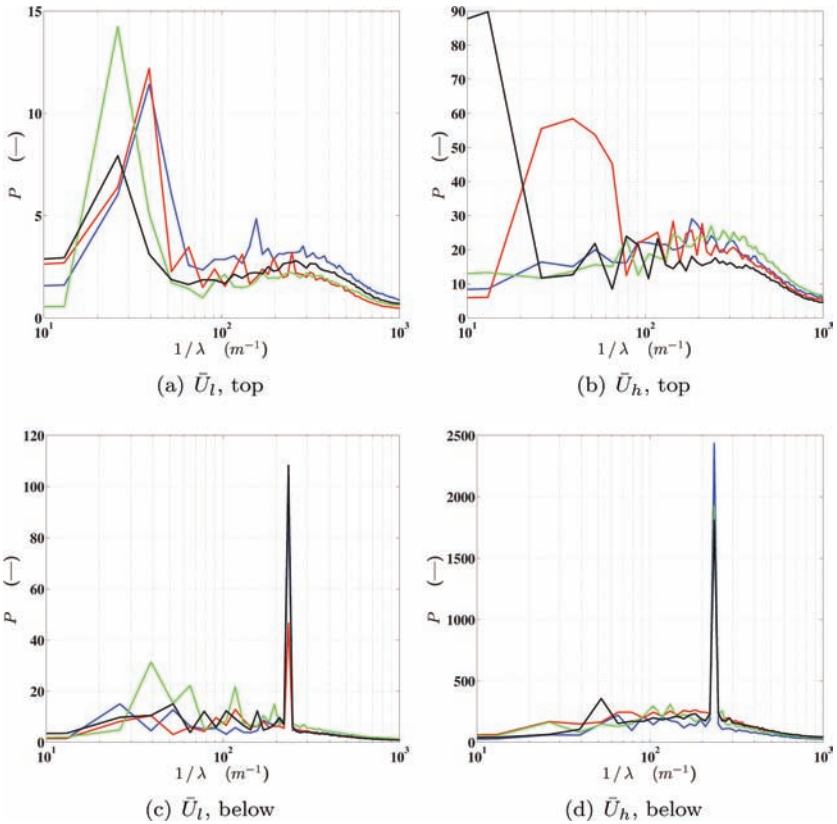

Figure 9. Wavenumber spectrum for velocity variations in horizontal direction above (a, b) and below (c, d) the filter grid. Test cases with $U_\infty = 18.8$ mm/s (a, c) and $U_\infty = 64.6$ mm/s (b, d). Fiber grammages are $w = 156$ g/m^2 (blue), $w = 469$ g/m^2 (red), $w = 1406$ g/m^2 (green) and $w = 1875$ g/m^2 (black).

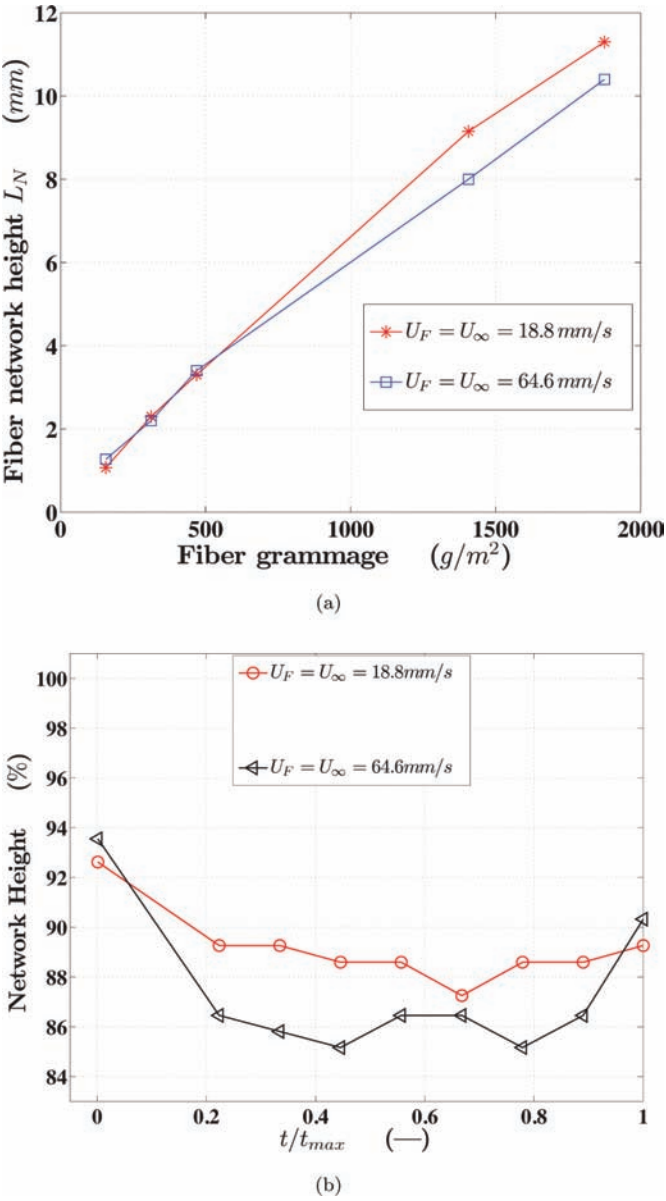

Figure 10. (a) Mean fiber network height during filtration as a function of grammage for high and low filtration velocities. (b) Relative fiber network height, before ($t = 0$), during and after filtration ($t = t_{max}$).

the original shape, although plastic deformation remains. This tendency is more evident for the lowest filtration velocity. This surprising observation could be explained by the fact that at lower filtration rate, the network is subjected to the compression force for much longer time, so creeping effects similar to those observed by could occur.

Figure 10(b) shows the measured network height averaged in time as a function of the fiber grammage. Here we see that differences between low and high filtration rates are more evident for higher grammages.

4 CONCLUSIONS

The flow and the pressure drop generated during filtration of a fiber suspension has been studied experimentally in this work. The initial fiber concentration was increased stepwise, a network was formed with a given *formation* velocity, and then filtration was performed with a defined *filtration* velocity over this steady network. Hence the resulting pressure drop and filtration rate were constant during the experiments, and statistics could be accurately computed. Pressure drop measurements and PIV of the filtration flow have been performed. Also, details of the network deformation during filtration were extracted by image processing.

A linear dependence of the pressure drop with the basis weight was found. A non-dimensional filtration resistance R was derived from Darcy's law that was found to be independent of filtration velocity and network thickness. Also, the formation velocity does not affect the pressure drop in our range of parameters.

The mean velocity field acquired with PIV were analyzed both qualitatively and quantitatively. Qualitatively, it is clear that velocity gradients are induced by the filter medium, and the characteristic scales of these gradients increases as soon as the first layer of fibers deposits on the network. Quantitative analysis of the mean flow field confirmed this impression but surprisingly, no influence of the filtration velocity on these scales was found. The scales of the velocity gradients go from 4mm (i.e., the mesh size) where no fibers are on the grid up to 8–20 mm as the thickness of the network increases. This means that velocity gradients exist on the size of a fiber length and could modify fiber orientation.

Analysis of the images acquired during filtration revealed that compression occurs both for low and high filtration velocities. Part of this compression is elastic, since the network tends to recover its original dimension once the filtration ends. However, a residual permanent deformation is observed. Permanent deformation was larger for the lowest filtration velocity. This might be explained by the fact that slowest filtration has a longer duration, thus creeping effects might occur.

This experiment establish a methodology to study the complex flow generated during filtration, and it could be extended to study influence of parameters such

as: material properties of fibers (stiffness, porosity, etc.) and geometrical properties (e.g. fiber length, cross sectional shape, etc.). Furthermore, with improved index-of-refraction matching and fluorescent particles, it might also be possible to study flow and transport of less elongated particles through the fiber network.

REFERENCES

1. G. Bellani. 'Velocity Measurements in a Fiber Suspension Flow: Formation of a Fiber Network.' Licentiate Thesis, Royal Institute of Technology, Stockholm, 2008.
2. R. Bürger, F. Concha and K. H. Karlsen. Phenomenological model of filtration processes: 1. Cake formation and expression. *Chemical Engineering Science*, **56**:4537–4553, Jan 2001.
3. F. Concha and R. Bürger. A century of research in sedimentation and thickening. *KONA Powder and Particle*, **20**:38–70, Jan 2002.
4. A. Gokce, M. Chohra, S. Advani and. Walsh. Permeability estimation algorithm to simultaneously characterize the distribution media and the fabric preform in vacuum assisted resin transfer molding process. *Composites Science and Technology*, **65**:2129–2139, Jan 2005.
5. Juergen Hoferer, Martin J. Lehmann, Edme H. Hardy, Joerg Meyer and Gerhard Kasper. Highly resolved determination of structure and particle deposition in fibrous filters by MRI. *Chem Eng Technol*, **29**(7):816–819, Jan 2006.
6. C. Holmqvist. 'Mechanical Modelling of Blade Forming and Drainage of Occulated Suspensions.' PhD Thesis, Royal Institute of Technology, Stockholm, Jan 2005.
7. G Jeffery. The motion of ellipsoidal particles immersed in a viscous fluid. *Proceedings of the Royal Society of London*. Series A, Jan 1922.
8. G. Kynch. A theory of sedimentation. *Transactions of the Faraday Society*, Jan 1952.
9. H. Liimatainen, S. Kokko, P. Rousu and J. Niinimaki. Effect of PCC filler on dewatering of fiber suspension. *Tappi J*, **5**(11):11–17, Jan 2006.
10. M. Lucisano and B. Norman. The forming and properties of quasi-random laboratory paper sheets. *Proceedings of International Paper Physics Conference, San Diego*, p. 11, July 2004.
11. F. Lundell, L. D. Söderberg and P. H. Alfredsson. Fluid mechanics of papermaking. *Annual Review of Fluid Mechanics*, **43**:195–217, Jan 2010.
12. N. N. Sayegh and T. O. Gonzalez. Compressibility of fiber mats during drainage. *J Pulp Pap Sci*, **21**(7):J255–J261, Jan 1995.
13. W. Sampson, J. McAlpin, H. Kropholler, and C. T. J. Dodson. Hydrodynamic smoothing in the sheet forming process. *Journal of Pulp and Paper Science*, Jan 1995.
14. F. Zhou, J. Alms and S. Advani. A closed form solution for ow in dual scale fibrous porous media under constant injection pressure conditions. *Composites Science and Technology*, **68**:699–708, Jan 2008.

Transcription of Discussion

EXPERIMENTAL STUDY OF FILTRATION OF FIBRE SUSPENSION

PART I

Gabriele Bellani,[1] *Fredrik Lundell*[1] *and L. Daniel Söderberg*[1,2]

PART II

Gabriele Bellani,[1] *Roland Bach,*[1] *Fredrik Lundell*[1] *and L. Daniel Söderberg*[1,2]

[1] Linné Flow Centre, KTH Mechanics, SE-100 44 Stockholm, Sweden
[2] Innventia AB, SE-114 86 Stockholm, Sweden

Kit Dodson University of Manchester, Mathematics

It was very nice to see those pictures. We worked on related things with much more primitive methods and it was brought to Oxford in 1965. The paper was called *The Detection and Cause of Layering in Paper*. At that time, we did not have the extremely good laser sheet light. We scratched the paint off the side of a transistor. It made it light sensitive and we had effectively a cafetière. For what this did was demonstrate that the fibres formed in a layered way and the additional part of the paper showed how to calculate the degree of layering. I don't see it mentioned, but it does say more or less what you have done, but using wood fibres.

Fredrik Lundell KTH Mechanics

Thank you very much. I can say that I am happy, that I am an experimentalist nowadays and not back then. The studies you did with the equipment you had is just amazing.

Discussion

Jean-Claude Roux Grenoble Institute of Technology

I would like to thank you for this very interesting presentation and I was very pleased to see your curve in the second case: Formation of a fibre network where you put the thickness of the fibrous network versus the fibre grammage. For both cases of speed and velocity 18.8mm/s and 64.6mm/s you get more or less the same slope. You probably know that in many modellings of the forming process on paper machines, we may assume that the fibrous mat, to a certain extent, has a solid consistency which is constant: whatever the increase of the pressure drop. On your pictures, you get this result which is very interesting because for the first time it's not an hypothesis, but a fact.

Fredrik Lundell

Thank you. In this context I would like to emphasize that this is filtration from a 0.5% suspension. If one is interested in thickening, there is a bit more work to do.

Joel Panek WestRock

I am not familiar with this area and the images and the graphics look fascinating. What is the biggest contribution of this work to the advances in our research? What do you think is the one or two things that we should take away from this work?

Fredrik Lundell

I think the big thing is probably the experiment as such. With this, we could also look at filler transported in the fibre mat. If we could find good ways to manipulate the adhesion between these fibres and some scaled filler particles, we could look at filler transport through the fibre web with different agglomerates etc. So, I think that if there is anything that is a long-term contribution to the field, except for things that were only hypothesized on, then it's the fact that we have an experiment where we can look at such things in a consistent manner.

Joel Panek

Okay. I guess the development of experimental techniques is directly observed.

Fredrik Lundell

Yes. Also, there is a community working with cut fishing line as model fibres and in that community our fibre ends are quite good.